Bitlis Eren Üniversitesi Fen Bilimleri Dergisi
BİTLİS EREN UNIVERSITY JOURNAL OF SCIENCE
ISSN: 2147-3129/e-ISSN: 2147-3188
VOLUME: 13 NO: 4 PAGE: 1047-1066 YEAR: 2024
DOI: 10.17798/bitlisfen.1500249

Comprehensive Energy and Exergy Analysis of a Pressurized Water Reactor Driven Multi-Stage Flash Desalination Plant

Erdem AKYÜREK[1], Tayfun TANBAY[1*]

[1]*Bursa Technical University, Faculty of Engineering and Natural Sciences, Department of Mechanical Engineering, Bursa, Türkiye*
(ORCID: 0000-0002-8856-2387) (ORCID: 0000-0002-0428-3197)

Keywords: Nuclear desalination, Multi-stage flash, Pressurized water reactor, Energy analysis, Exergy analysis.

Abstract

Nuclear energy-based seawater desalination is an environmentally friendly freshwater production approach. This study introduces a novel thermodynamic model integrating a pressurized water reactor's (PWR) secondary cycle with a multi-stage flash (MSF) desalination facility to enhance freshwater production. The impacts of the design and operating conditions on thermal efficiency, utilization factor, gain output ratio, exergy efficiency, coefficient of ecological performance for cogeneration and exergy destruction factor are investigated. Results reveal that a higher live steam temperature and a reheater mass flow rate ratio is preferable for a better nuclear desalination performance. A larger freshwater production capacity is preferable for a better utilization factor, however increasing the capacity tends to decrease thermal efficiency, coefficient of ecological performance for cogeneration and exergy destruction factor. The selection of steam extraction location is important for very large scale plants, and the outlet of moisture separator is determined to be the best option. Parametric analysis shows that plant's performance can be significantly improved by adjusting the design conditions. Thermal and exergy efficiencies of an optimized plant configuration are 3.01% and 4.70% higher, respectively as compared to a base plant. It is also found that steam generator and MSF unit cause 3.2% and 82% of the total irreversibility rate of PWR's secondary cycle and MSF facility, respectively, and have the highest irreversibility rates for these sections of the plant.

1. Introduction

With the impact of industrialization, agricultural production and rapid population growth, the demand for freshwater is constantly increasing. Water pollution and arid climatic conditions reduce the per capita water supply worldwide and cause water scarcity. The water crisis has a significant negative impact on the development of countries owing to its influence on economic activities and the people's quality of life [1]. Approximately 97.5% of the water available on the Earth's surface is sea and ocean water, while 2.5% is freshwater including glaciers, groundwater, streams and lakes, and only less than 1% of freshwater is easily accessible and usable [2]. In a United Nations report [3], it is stated that the world's water stress level is about 18% in 2018. According to the report, approximately 10% of the global population reside in areas with water shortages, and it is pointed out that the requirement for water will increase in the coming years due to the impact of population density.

Seawater desalination, which is an option to meet freshwater demand, is the process of separating purified water from seawater having high salt concentration by consuming energy. The required energy for desalination processes can be provided from fossil-based, renewable or nuclear energy. Compared to alternative energy sources nuclear power plants (NPPs) have the largest capacity factor

*Corresponding author: tayfun.tanbay@btu.edu.tr
Received:12.06.2024, Accepted: 10.12.2024

[4, 5]. The high availability of nuclear energy used in desalination applications can eliminate the energy storage requirement problems of renewables. In addition, nuclear power is advantageous to fossil-fueled plants since it can completely eliminate CO_2 emissions. Fossil fuel-driven MSF and multi-effect distillation (MED) desalination plants emit approximately 22.5 kg CO_2 and 17.5 kg CO_2 per 1 m^3 of freshwater produced, respectively [6]. It is possible to significantly reduce CO_2 emissions by utilizing clean energy sources such as nuclear for the desalination of seawater [7].

In a nuclear reactor driven desalination plant, the fission energy of the reactor is converted into thermal energy, and part of this energy is used for the desalination of seawater. MSF, MED and thermal vapor compression (TVC) are used as distillation processes while reverse osmosis (RO) is utilized as a membrane process in nuclear desalination facilities. RO, MSF and MED processes account for 70%, 18% and 7% of the global installed desalination capacity, respectively [8]. MSF, MED and RO desalination processes consume total energy in the range of $18.3-28.5\ \mathrm{kWh/m^3}$, $14.2-21.6\ \mathrm{kWh/m^3}$ and $4-6\ \mathrm{kWh/m^3}$, respectively [9]. Although the energy use of MSF is high, it can be operated with high capacity and its maintenance is easier [10], and also MSF has a high water quality in the range $2-10$ ppm [9].

Seawater desalination and the integration of these processes to nuclear energy have been the topic of many technical and/or economic studies. Four different coupling alternatives of cogeneration systems were analyzed with Desalination Thermodynamic Optimization Program (DE-TOP) software developed by the International Atomic Energy Agency (IAEA) [11]. IAEA also developed the Desalination Economic Evaluation Program (DEEP) for the economic evaluation of desalination plants driven by nuclear, fossil and renewable sources [12]. An economic analysis of the MSF process coupled to nuclear and fossil fueled cogeneration plants was performed by Faibish and Ettouney [13]. The impacts of production capacity and top brine temperature (TBT) on the cost were investigated, and it was found that the nuclear-based MSF produced freshwater with a cost that is lower than fossil fuel-based distillation. In another study, the costs of water desalinated by MSF, MED and RO to meet the potable water requirement in two different site conditions in Libya were determined and compared with fossil-based desalination [14].

The integration of International Reactor Innovative and Secure plant to MSF and RO for nuclear desalination was considered by [15]. Economic analysis revealed that the plant cost of the nuclear MSF desalination plant was minimized at a TBT of $82-83$℃. Adak and Tewari [16] investigated the coupling of an MSF facility to a pressurized heavy water reactor (PHWR), and found that a water production rate of $4500\ \mathrm{m^3/day}$ with a gain output ratio (GOR) of 9 can be obtained at the expense of a 3.3 MW decrease in the net power output of the NPP. A technical and safety study on the thermal coupling aspects for isolation purposes of this plant was presented by [17]. Safety features were evaluated to prevent any radioactivity entering the product water in the integrated plant that employed two isolation heat exchangers. Tian et al. [18] compared the electricity and freshwater costs of nuclear and fossil fuel powered MSF desalination plants. The parameters considered in the assessment were the discount rate, fossil fuel price, power plant investment and desalination plant size. The analysis showed that the nuclear option was economically advantageous to fossil fuel based desalination.

The exergy analysis of a MSF desalination plant was performed by Kahraman and Cengel [19], which showed that the MSF unit cause the largest irreversibility and its exergetic performance could be improved by utilizing more flashing stages. The thermal coupling of MSF and MED facilities to a system-integrated modular advanced reactor (SMART) was studied in [20]. Three coupling techniques were compared, and it was found that the heat pipe loop was the optimum plant integration method. Thermoeconomic multiobjective optimization of a PWR coupled to an MSF plant was carried out to minimize the product water and electricity costs [21, 22]. Thermoflex simulator was used for thermodynamic modelling, and the optimization was carried out with a genetic algorithm. Alonso et al. [23] presented a comparative economic analysis by coupling MSF, MED, RO, MSF-RO and MED-RO with two different PWRs. The electricity and freshwater costs of cogeneration applications were determined for three different discount rates. MED was found to be less expensive than MSF and the coupling of RO to MSF and MED would improve the competitiveness of these thermal desalination technologies.

Yan et al. [24] examined the integration of a high-temperature gas cooled reactor (HTGR) to an MSF plant. The analysis revealed that an incrementally loaded MSF system would increase the freshwater production by 45% and use of reactor thermal power by 16% compared to the conventional MSF desalination. The techno-economic evaluation of cogeneration options for a small modular reactor (SMR) coupled to MSF, MED and RO were carried out by [25]. Three different coupling strategies of the

MSF and MED with the reactor were considered, and the relationship between electricity and freshwater outputs was investigated. The results indicated that RO causes the least cost and the SMR provided flexible operation for all desalination processes. Exergetic and thermo-economic analyses of SMART reactor-based MSF and MED-TVC desalination are performed by Priego et al. [26]. The effect of steam extraction nodes from the secondary cycle of the reactor on the cost of fresh water is assessed for three gain output ratios and four discount rates. Techno-economic analysis of two SMRs, namely SMART and CAREM (Central Argentina de Elementos Modulares), was carried out by Khan et al. [27] for nuclear desalination with MSF, MED and RO. In another techno-economic analysis, the Karachi NPP was considered for nuclear desalination with MSF, MED, RO, MSF-RO and MED-RO approaches [28]. The results indicated that MED was economically advantageous.

Polat and Dinçer [29] compared MSF, MED, RO, MSF-RO and MED-RO based nuclear desalination methods. Akkuyu NPP, which is a Water-Water Energy Reactor (WWER) under construction, is considered as the heat and/or electricity source for desalination and DEEP is used to determine the freshwater production costs. The integration of an experimental gas cooled reactor to MSF for nuclear desalination was studied by Dewita et al. [30]. The impact of steam extraction nodes on freshwater production capacity was analyzed by considering two options. Sadeghi et al. [31] investigated the integration of the Bushehr NPP with hybrid MSF-RO and MED-RO desalination processes for three coupling options and performed the techno-economic analysis of the plant. The total cost of freshwater was determined, and it was found that extracting steam from the condenser outlet was the best alternative. Finally, in a recent work [32], an exergoeconomic analysis of a PWR coupled to MSF and RO for nuclear desalination was carried out. Aspen HYSYS software was used for the modelling of the PWR's secondary cycle.

The abovementioned studies do not present a thermodynamic model that involves both the nuclear reactor's energy conversion system and MSF facility of a nuclear desalination plant. Therefore, in order to fill this research gap, this paper introduces a novel thermodynamic model integrating a PWR's secondary cycle with an MSF desalination facility to produce electricity and freshwater, and presents a comprehensive thermodynamic analysis of the cogeneration system. The novelties of this study are:

- A detailed thermodynamic model considering the components of both the PWR's secondary cycle and MSF facility is built for a comprehensive energy and exergy analysis of the plant.
- The impacts of the design and operating conditions of i) reactor thermal power, ii) live steam temperature, iii) reheater mass flow rate ratio, iv) reheater temperature, v) process steam extraction node, vi) freshwater production capacity, vii) TBT, viii) MSF unit throttling mass flow rate ratio ix) seawater temperature, and x) seawater salinity on the objective functions of i) thermal efficiency, ii) utilization factor, iii) gain output ratio, iv) exergy efficiency, v) coefficient of ecological performance, and vi) exergy destruction factor are investigated.

2. System Description

The detailed schematic representation of the PWR driven MSF desalination plant is illustrated in Figure 1. Nuclear facility is composed of two cycles. Fission energy of the nuclear reactor is transferred to liquid water circulating in the primary loop, which is coupled to the secondary loop through a steam generator (SG). Steam is obtained at the outlet of the cold side of the SG (state 4) by heat transfer from the primary loop. The majority of the steam enters the high-pressure turbine (HPT) to produce electrical power output, while the rest is directed to reheater (RH) for reheating the steam to low-pressure turbine (LPT) inlet conditions. The moisture separator (MS) transfers the liquid water to a feedwater heater (FWH) to improve the service life of the plant. Steam leaving the RH enters the LPT to produce additional power and the expanded steam then enters the condenser (C). Secondary cycle contains seven FWHs to increase the thermal efficiency of the plant and the pumps (P) are utilized to increase the pressure of water to SG inlet condition. FWHs also provide flexibility in operation of the plant by enabling the transfer of process steam to the MSF facility at different conditions. Green lines represent the possible steam extraction locations for desalination. Steam is extracted from only one of the states of 52, 53, …, 63 and returns the cycle through C.

The secondary cycle of the PWR is coupled to the MSF facility through a heat exchanger (HX). In addition to transferring the energy of the process steam to the MSF facility, the HX acts as an isolation loop that prevents the contamination of both nuclear and MSF cycles. The desalination facility includes an MSF unit consisting of heat recovery and heat rejection sections with multiple horizontal in-line evaporators, a brine heater, a throttling valve, pumps and a vacuum system. Each evaporator has a flashing chamber where seawater evaporates and a condensation section where the pure water is distilled.

Seawater entering the facility at state 0 is first directed to the condensation section of the evaporators to condense the pure water vapor and then exits through the heat rejection section of MSF unit at state 69. Part of the seawater is discharged back to the sea, while the remainder (state 70) is throttled and utilized as make-up feedwater in the MSF unit. The portion of the feedwater leaving the heat rejection section at state 74 is heated by recirculation to the evaporators in the heat recovery section. The feedwater then enters the brine heater (BH), and it is heated to the TBT with the process heat of the steam that is extracted from the PWR's secondary loop through the isolation HX. The heated feedwater enters the flash chamber of the first evaporator at state 77, and it is vaporized due to pressure drop. The pure water vapor passes through the demister, which prevents the passage of the salt, and then it condenses by transferring heat to the seawater in the condensation section and is collected on the distillation tray. This operation is repeated in each stage of the MSF unit and the product water leaves the desalination facility at state 72. The high-salinity brine water leaves the MSF unit at state 73, and it is directed back to the sea.

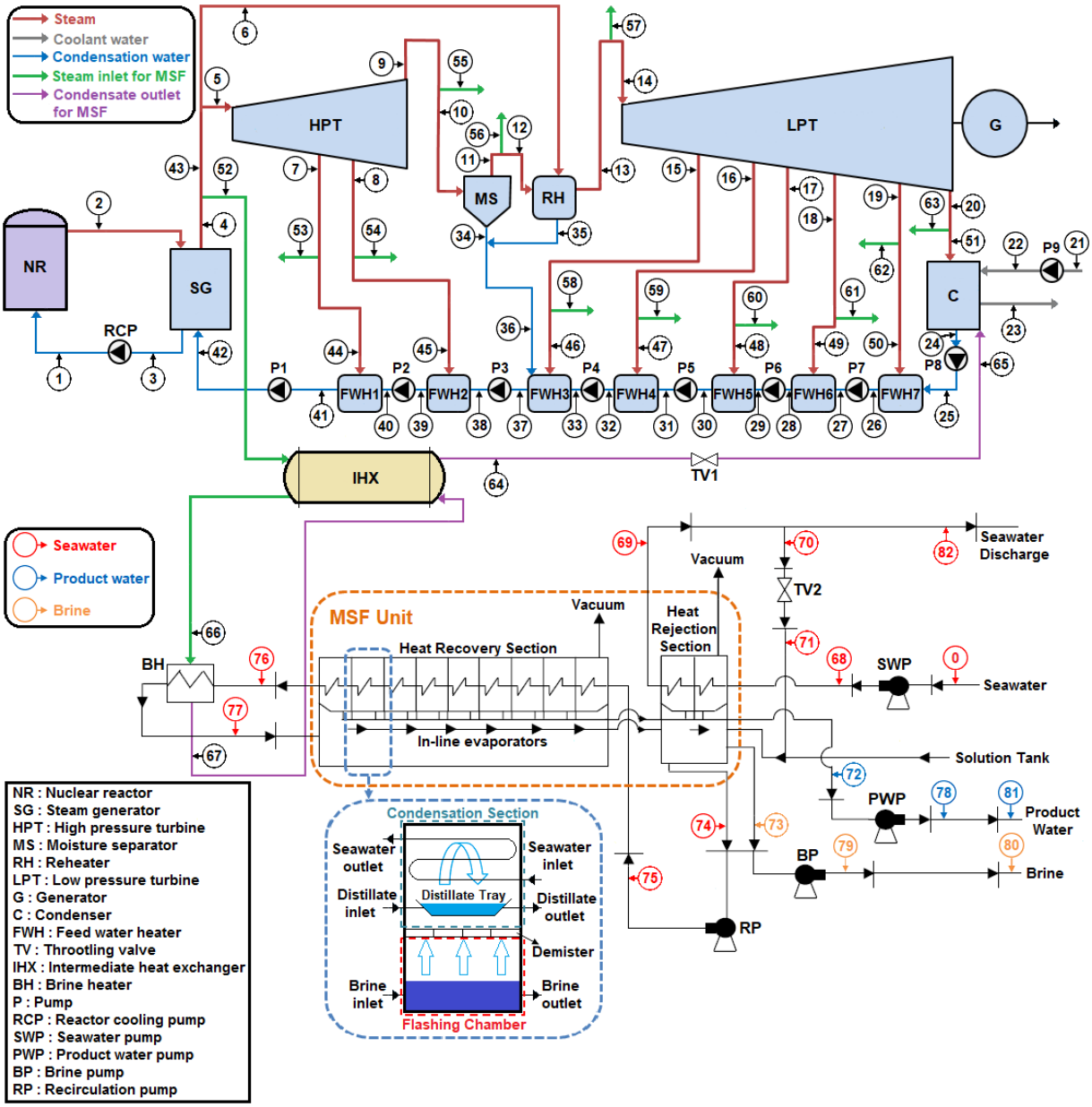

Figure 1. Illustration of the PWR driven MSF desalination plant (adapted from [11, 19]).

The plant design presented in Figure 1 has several advantages over alternative configurations. First of all, the nuclear-driven cogeneration system completely eliminates the CO_2 that would be emitted from a fossil fuel-based cogeneration plant, and hence it offers an environmental benefit. The design is also

advantageous to renewable-based plants since nuclear energy is superior to renewables in terms of capacity factor. The use of PWR instead of alternative reactor technologies such as PHWR, SMART and HTGR is another advantage of the configuration presented in Figure 1, since PWRs are the most widely utilized reactors in the nuclear industry. Therefore, the PWR technology is more accessible for nuclear desalination as compared to alternative reactors. As for the choice of MSF process for desalination, it is advantageous to alternative desalination approaches with its large production capacity and high water quality. Freshwater with a high level of purity is a valuable commodity since it can be utilized as an input for a hydrogen production facility employing electrolysis as the production method.

3. Modeling of the System

In this section, first the main assumptions employed in the modeling of the plant are given. Then, the energy-exergy analyses of the nuclear desalination plant are presented. Following the definition of saline water properties, finally, the objective functions are introduced.

3.1. Assumptions

The main assumptions for the modeling of the nuclear desalination plant are as follows:

- All processes are steady-flow and hence the parametric analyses are time-independent.
- The change in kinetic and potential energies is neglected.
- All plant components are adiabatic except the MSF unit.
- MSF unit is nonadiabatic [19, 33]. Exergy balance equations presented in Ref [19] for the MSF unit, and in Ref [33] for the heat recovery and rejection sections indicate that the MSF unit is adiabatic. However, calculations based on the thermodynamic data presented in Table 1 of Ref [19] and in Tables 4 and 5 of Ref [33] show that the component is nonadiabatic.
- There is no frictional pressure loss in the cycle.
- Isentropic efficiencies are used to factor in the irrevesibilities of turbines, pump and generator.
- Water leaves the SG and MS at state 11 as a saturated vapor, while it leaves the MS as a saturated liquid at state 34.
- Liquid water enters nuclear facility through the condenser for cooling at state 21 and the MSF facility at state 0 at ambient temperature.
- A temperature difference of 5℃ is present in both sides of C and the inlet and outlet of the cold side of C (i.e., $T_{24} = T_{23} + 5℃$ and $T_{23} = T_{22} + 5℃$) [11].
- Steam extraction from PWR's secondary loop is made through only one of the locations 52, …, 63.
- Desalination capacity is a function of the TBT, T_{77} [34]. The amount of product water, i.e., $\dot{m}_{72}$, depends on the TBT as

$$\dot{m}_{72} = \dot{m}_{74}\left[1 - (1 - y)^{(TBT - T_{73})/\Delta T_{st}}\right] \quad (1)$$

where $\dot{m}_{74}$ is the recycle brine mass flow rate, y is the ratio of sensible heat to latent heat of salt-water mixture in the MSF unit, ΔT_{st} is the temperature decrease of the brine per MSF unit stage and T_{73} is the brine temperature.

- The feed seawater mass flow rate to the MSF unit, i.e., $\dot{m}_{71}$, is related to the product water mass flow rate as [34]

$$\dot{m}_{71} = \dot{m}_{72}\frac{Sal_{73}}{Sal_{73} - Sal_{71}} \quad (2)$$

where Sal_{71} and Sal_{73} are the salinities of the seawater and brine, respectively. The brine salinity is limited by environmental regulations.

- The temperature of the seawater increases by 8℃ and its pressure decreases by 30% in the heat rejection section of the MSF unit (i.e., $T_{69} = T_0 + 8℃$ and $P_{69} = 0.7P_{68}$) [19]. Also, there exists a temperature difference of 5℃ on the cold side of the BH (i.e., $T_{77} = T_{76} + 5℃$).

3.2. Energy and Exergy Analysis

The energy analysis of the plant is carried out by applying the conservation of mass and energy equations to plant components

$$\sum_{in} \dot{m} = \sum_{out} \dot{m} \quad (3)$$

$$\dot{Q}_{in} + \dot{W}_{in} + \sum_{in} \dot{m}h = \dot{Q}_{out} + \dot{W}_{out} + \sum_{out} \dot{m}h \quad (4)$$

where $\dot{m}$ is the mass flow rate, $\dot{Q}$ and $\dot{W}$ are the rates of heat and work transfer, respectively, and h represents the enthalpy. Eqs. (3) and (4) yield the heat transfer rate from the primary cycle of nuclear plant to the secondary cycle through SG ($\dot{Q}_{SG}$), the heat

transfer rate from C, the power production rates of HPT and LPT ($\dot{W}_{HPT}$ and $\dot{W}_{LPT}$), the power consumption rates of Ps ($\dot{W}_P$), heat transfer rate from the nuclear plant to MSF plant through HX ($\dot{Q}_p$) and heat loss rate of the MSF unit ($\dot{Q}_{MSF}$). The energy balance equations are presented in Table 1.

Table 1. Energy balance equations for the components of the nuclear desalination plant.

Component	Energy balance equations
	Nuclear plant
SG	$\dot{Q}_{SG} = \dot{m}_4(h_4 - h_{42})$
HPT	$\dot{W}_{HPT} = \dot{m}_5 h_5 - (\dot{m}_7 h_7 + \dot{m}_8 h_8 + \dot{m}_9 h_9)$
MS	$\dot{m}_{10} h_{10} = \dot{m}_{11} h_{11} + \dot{m}_{34} h_{34}$
RH	$\dot{m}_6(h_6 - h_{35}) = \dot{m}_{12}(h_{14} - h_{12})$
LPT	$\dot{W}_{LPT} = \dot{m}_{14} h_{14} - (\dot{m}_{15} h_{15} + \dot{m}_{16} h_{16} + \dot{m}_{17} h_{17} + \dot{m}_{18} h_{18} + \dot{m}_{19} h_{19})$
C	$\dot{m}_{22} h_{22} + \dot{m}_{51} h_{51} + \dot{m}_{65} h_{65} = \dot{m}_{23} h_{23} + \dot{m}_{24} h_{24}$
Ps	$\dot{W}_{P,j} = \dot{m}_{in,j}(h_{out,j} - h_{in,j}), \quad j = 1, \dots, 9$
FWHs	$\dot{m}_{out,j} h_{out,j} = \sum_{in,j} \dot{m} h, \quad j = 1, \dots, 7$
IHX	$\dot{Q}_p = \dot{m}_i(h_i - h_{64}) = \dot{m}_{66}(h_{66} - h_{67}), \ i = 52,53, \dots, \text{or } 63$
Flow mixing	$\dot{m}_{34} h_{34} + \dot{m}_{35} h_{35} = \dot{m}_{36} h_{36}$
TV1	$h_{65} = h_{64}$
	Desalination plant
SWP	$\dot{W}_{SWP} = \dot{m}_{68}(h_{68} - h_0)$
TV2	$h_{71} = h_{70}$
MSF unit	$\dot{Q}_{MSF} = (\dot{m}_{68} h_{68} + \dot{m}_{71} h_{71} + \dot{m}_{75} h_{75} + \dot{m}_{77} h_{77}) - (\dot{m}_{69} h_{69} + \dot{m}_{72} h_{72} + \dot{m}_{73} h_{73} + \dot{m}_{74} h_{74} + \dot{m}_{76} h_{76})$
BH	$\dot{m}_{76}(h_{77} - h_{76}) = \dot{m}_{66}(h_{66} - h_{67})$
PWP	$\dot{W}_{PWP} = \dot{m}_{72}(h_{78} - h_{72})$
BP	$\dot{W}_{BP} = \dot{m}_{73}(h_{79} - h_{73})$
RP	$\dot{W}_{RP} = \dot{m}_{74}(h_{75} - h_{74})$

The irreversibility rates of plant components are determined by applying the exergy balance equation

$$\left(1 - \frac{T_0}{T_b}\right)\dot{Q}_{in} + \dot{W}_{in} + \sum_{in} \dot{X}_i - \left(1 - \frac{T_0}{T_b}\right)\dot{Q}_{out} - \dot{W}_{out} - \sum_{out} \dot{X}_i - \dot{X}_{dest} = 0 \quad (5)$$

where $\dot{X}_{dest}$ is the exergy destruction rate, $\dot{X}_i$ is the exergy flow rate, while T_0 and T_b are the dead state and average boundary temperature, respectively. Eq. (5) can be used to determine the exergy destruction rates of nuclear desalination plant components, and the equations are presented in Table 2, where T_{SG} and T_{MSF} are the average boundary temperatures of SG and MSF unit, respectively. Exergy flow rate is defined as

$$\dot{X}_i = \dot{m}[h_i - h_0 - T_0(s_i - s_0)] \quad (6)$$

where h_0 and s_0 are the enthalpy and entropy at T_0.

Table 2. Exergy balance equations for the components of the nuclear desalination plant.

Component	Exergy balance equations
	Nuclear plant
SG	$\dot{X}_{dest,SG} = \dot{X}_{42} - \dot{X}_4 + \left(1 - \frac{T_0}{T_{SG}}\right)\dot{Q}_{SG}$
HPT	$\dot{X}_{dest,HPT} = \dot{X}_5 - \dot{X}_7 - \dot{X}_8 - \dot{X}_9 - \dot{W}_{HPT}$
MS	$\dot{X}_{dest,MS} = \dot{X}_{10} - \dot{X}_{11} - \dot{X}_{34}$
RH	$\dot{X}_{dest,RH} = \dot{X}_6 + \dot{X}_{12} - \dot{X}_{13} - \dot{X}_{35}$
LPT	$\dot{X}_{dest,LPT} = \dot{X}_{14} - \dot{X}_{15} - \dot{X}_{16} - \dot{X}_{17} - \dot{X}_{18} - \dot{X}_{19} - \dot{W}_{LPT}$
C	$\dot{X}_{dest,C} = \dot{X}_{22} + \dot{X}_{51} + \dot{X}_{65} - \dot{X}_{23} - \dot{X}_{24}$
Ps	$\dot{X}_{dest,P,j} = \dot{X}_{in,j} - \dot{X}_{out,j} + \dot{W}_{P,j}, \quad j = 1,\dots,9$
FWHs	$\dot{X}_{dest,FWH,j} = \sum_{in,j} \dot{X}_i - \dot{X}_{out,j}, \quad j = 1,\dots,7$
IHX	$\dot{X}_{dest,IHX} = \dot{X}_i + \dot{X}_{67} - \dot{X}_{64} - \dot{X}_{66}, \ i = 52,53,\dots,\text{or } 63$
Flow mixing	$\dot{X}_{dest,mix} = \dot{X}_{34} + \dot{X}_{35} - \dot{X}_{36}$
TV1	$\dot{X}_{dest,TV1} = \dot{X}_{64} - \dot{X}_{65}$
	Desalination plant
SWP	$\dot{X}_{dest,SWP} = \dot{X}_0 - \dot{X}_{68} + \dot{W}_{SWP}$
TV2	$\dot{X}_{dest,TV2} = \dot{X}_{70} - \dot{X}_{71}$
MSF unit	$\dot{X}_{dest,MSF} = \dot{X}_{68} + \dot{X}_{71} + \dot{X}_{75} + \dot{X}_{77} - \dot{X}_{69} - \dot{X}_{72} - \dot{X}_{73} - \dot{X}_{74} - \dot{X}_{76} - \left(1 - \frac{T_0}{T_{MSF}}\right)\dot{Q}_{MSF}$
BH	$\dot{X}_{dest,BH} = \dot{X}_{66} + \dot{X}_{76} - \dot{X}_{67} - \dot{X}_{77}$
PWP	$\dot{X}_{dest,PWP} = \dot{X}_{72} - \dot{X}_{78} + \dot{W}_{PWP}$
BP	$\dot{X}_{dest,BP} = \dot{X}_{73} - \dot{X}_{79} + \dot{W}_{BP}$
RP	$\dot{X}_{dest,RP} = \dot{X}_{74} - \dot{X}_{75} + \dot{W}_{RP}$
SW-Cooling	$\dot{X}_{dest,SW-Cooling} = \dot{X}_{69} - \dot{X}_{82}$
B-Cooling	$\dot{X}_{dest,B-Cooling} = \dot{X}_{73} - \dot{X}_{80}$
PW-Cooling	$\dot{X}_{dest,B-Cooling} = \dot{X}_{78} - \dot{X}_{81}$

3.3. Saline Water Properties

Desalination process alters the salinity of the feedwater and produces three streams as product, brine and discharge waters with different salinities. Therefore, the thermodynamic properties of the working fluid of the desalination plant have to be determined by considering it as a water-salt mixture. Enthalpy and entropy of such a mixture are determined by [19].

$$h_i = mf_{s,i}h_{s,i} + mf_{w,i}h_{w,i}, \tag{7}$$

$$s_i = mf_{s,i}s_{s,i} + mf_{w,i}s_{w,i} - \left(\frac{R_u}{M_{sw,i}}\right)\left(x_{s,i}\ln x_{s,i} + x_{w,i}\ln x_{w,i}\right) \tag{8}$$

where $i = 68,69,\dots,82$, mf is the mass fraction, x is the mole fraction, R_u is the universal gas constant and M is the molar mass, while the subscripts sw, s and w denote seawater, salt and water, respectively. The mass fraction of salt is expressed in terms of the salinity (Sal) of seawater having the unit ppm, and the mass fraction of water is:

$$mf_{s,i} = Sal_i(ppm) \times 10^{-6} \tag{9}$$

$$mf_{w,i} = x_{w,i}\frac{M_w}{M_{sw,i}} \tag{10}$$

The molar fractions of salt and water and the molar mass of saline water are determined by

$$x_{s,i} = \frac{M_w}{M_s\left(\frac{1}{mf_{s,i}} - 1\right) + M_w} \quad (11)$$

$$x_{w,i} = 1 - x_{s,i} \quad (12)$$

$$M_{sw,i} = x_{s,i}M_s + x_{w,i}M_w \quad (13)$$

Salt is an incompressible substance and its enthalpy and entropy are independent of pressure. On the other hand, these thermodynamic properties are functions of temperature and the temperature dependence of salt's enthalpy and entropy can be expressed as

$$h_{s,i} = h_{s,ref} + c_{p,s}\left(T_i - T_{ref}\right) \quad (14)$$

$$s_{s,i} = s_{s,ref} + c_{p,s} ln\left(\frac{T_i}{T_{ref}}\right) \quad (15)$$

where $c_{p,s}$ is the specific heat of salt, T_{ref} is a reference temperature and $h_{s,ref}$ and $s_{s,ref}$ are the corresponding enthalpy and the entropy values of salt. For $T_{ref} = 35℃$, $h_{s,ref} = 29.288\, kJ/kg$, $s_{s,ref} = 0.1009\, kJ/kgK$, while $c_{p,s} = 0.8368\, kJ/kgK$.

3.4. Objective Functions

The energetic performance of the nuclear desalination plant is investigated through three objective functions, namely thermal efficiency, utilization factor and gain output ratio defined as

$$\eta_{th} = \frac{\dot{W}_{net}}{\dot{Q}_{SG}} \quad (16)$$

$$\epsilon_u = \frac{\dot{W}_{net} + \dot{Q}_p}{\dot{Q}_{SG}} \quad (17)$$

$$GOR = \frac{\dot{m}_{distilled}}{\dot{m}_{steam}} = \frac{\dot{m}_{72}}{\dot{m}_{66}} \quad (18)$$

respectively. $\dot{Q}_{SG}$ and $\dot{Q}_p$ are given in Table 1 and $\dot{W}_{net}$ is the net electrical power output of the plant:

$$\dot{W}_{net} = \eta_{GEN}\left(\dot{W}_{HPT} + \dot{W}_{LPT}\right) - \left(\sum_{j=1}^{9} \dot{W}_{P,j} + \dot{W}_{SWP} + \dot{W}_{PWP} + \dot{W}_{BP} + \dot{W}_{RP}\right) \quad (19)$$

In Eq. (19), $\dot{m}_{72}$ and $\dot{m}_{66}$ represent the mass flow rates of the product water and steam for BH, respectively.

The exergetic performance of the plant is investigated through exergy efficiency, ecological coefficient of performance for cogeneration and exergy destruction factor

$$\eta_{ex} = \frac{\dot{W}_{net} + \dot{X}_p}{\dot{X}_{SG}} \quad (20)$$

$$ECOP_{cog} = \frac{\dot{W}_{net} + \dot{X}_p}{\dot{X}_{dest,tot}} \quad (21)$$

$$f_{ed} = \frac{\dot{X}_{dest,tot}}{\dot{X}_{SG}} \quad (22)$$

where $\dot{X}_{dest,tot}$ is the total exergy destruction rate of the plant, while $\dot{X}_p$ is the exergy of process heat and $\dot{X}_{SG}$ is the exergy of heat transferred through the SG:

$$\dot{X}_p = \dot{X}_i - \dot{X}_{64}, \quad i = 52,53, \dots, \text{or } 63 \quad (23)$$

$$\dot{X}_{SG} = \left(1 - \frac{T_0}{T_{SG}}\right)\dot{Q}_{SG} \quad (24)$$

It should be noted that although η_{ex}, $ECOP_{cog}$ and f_{ed} are exergetic performance indicators, these functions focus on different characteristics of the plant. Also, the objective functions have been normalized as follows in order to more clearly show the influence of the variables on the performance of the plant:

$$\bar{f} = \frac{f}{f_{max}} \quad (25)$$

where $f \equiv \eta_{th}, \epsilon_u, GOR, \eta_{ex}, ECOP_{cog}, f_{ed}$.

4. Results and Discussion

In this section, the comprehensive energy and exergy analysis of the PWR driven MSF desalination plant is presented. Thermal efficiency, utilization factor, gain output ratio, exergy efficiency, ecological coefficient of performance for cogeneration and exergy destruction factor are considered as objective functions to investigate the impacts of reactor thermal power ($\dot{Q}_{SG}$), live steam temperature (T_4), RH mass flow rate ratio (α_{RH}) and temperature (T_{14}), process steam extraction node (i_{ext}), freshwater production capacity ($\dot{m}_{72}$), top brine temperature (T_{77}), MSF unit throttling mass flow rate ratio (α_{TV2}), seawater temperature (T_0) and salinity (Sal_0) on the energetic and exergetic performance of the plant. An in-house code is developed with MATHEMATICA 11 to carry out the calculations, and JANAF data [35] is used for the thermophysical properties of water.

Tables 3 and 4 present the values of the design parameters and dead state properties of seawater when they are not considered as a variable in analyses, and the isentropic efficiencies of the components for PWR's secondary cycle and MSF facility, respectively. The mass flow rate ratio presented in Table 3 is defined as $\alpha_i = \dot{m}_i/\dot{m}_4$ with $\alpha_{RH} = \dot{m}_6/\dot{m}_4$, while the mass flow rate ratio of TV2 is $\alpha_{TV2} = \dot{m}_{70}/\dot{m}_{82}$.

Table 3. Main design parameters of the PWR secondary cycle.

Parameter	Value	Parameter	Value
$\dot{Q}_{SG}$	3300 MW	P_7	2600 kPa
T_{SG}	346.85℃	P_8	1600 kPa
T_4	277℃	P_{14}	1120 kPa
T_{14}	255℃	P_{15}	880 kPa
α_{RH}	0.06	P_{16}	450 kPa
i_{ext}	52	P_{17}	200 kPa
α_7	0.055	P_{18}	90 kPa
α_8	0.05	P_{19}	30 kPa
α_{15}	0.04	P_{22}	200 kPa
α_{16}	0.034	η_{HPT}	0.85
α_{17}	0.034	η_{LPT}	0.83
α_{18}	0.034	η_P	0.85
α_{19}	0.026	η_{GEN}	0.98

Table 4. Main design parameters of the MSF facility.

Parameter	Value	Parameter	Value
$\dot{m}_{74}$	3600 kg/s	P_{68}	168 kPa
ΔT_{st}	3℃	P_{71}	10 kPa
TBT	89.85℃	P_{75}	635 kPa
T_{72}	26℃	P_{78}	578 kPa
y	0.005	P_{79}	292 kPa
α_{TV2}	0.9	Sal_0	38000 ppm
T_0	20℃	Sal_{75}	65000 ppm
P_0	101.325 kPa	Sal_{78}	0.01 ppm
η_P	0.85	Sal_{79}	70000 ppm

Figure 2 shows the effect of reactor thermal power and live steam temperature on the objective functions related to the energetic and exergetic performance of the plant. Increasing $\dot{Q}_{SG}$ causes to improve η_{th}, $ECOP_{cog}$ and f_{ed}, and it has a negative impact on ϵ_u while the variation in η_{ex} is negligible. $\dot{Q}_{SG}$ has the largest effect on $ECOP_{cog}$ and f_{ed}. An increase of 0.2 GW changes these functions by 0.4%. A higher live steam temperature tends to increase the performance of the nuclear desalination plant. Performance indicators are more sensitive to the variation in T_4 as compared to the variation in $\dot{Q}_{SG}$. For instance, $ECOP_{cog}$ is enhanced by 13% when T_4 is increased by 18 ℃.

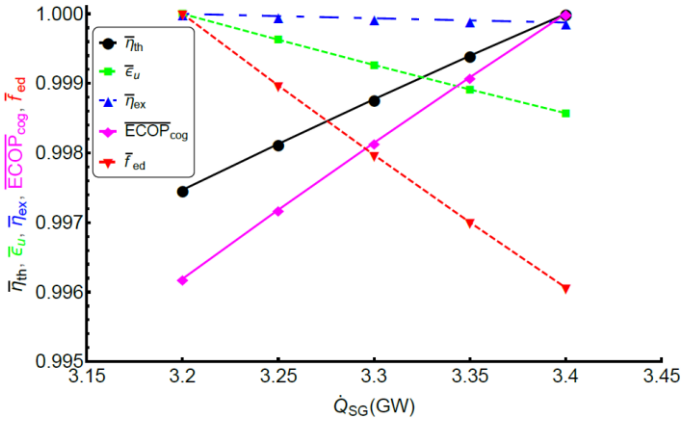

(a)

Figure 2. Impact of (a) Q ̇_SG and (b) T_4 on the objective functions

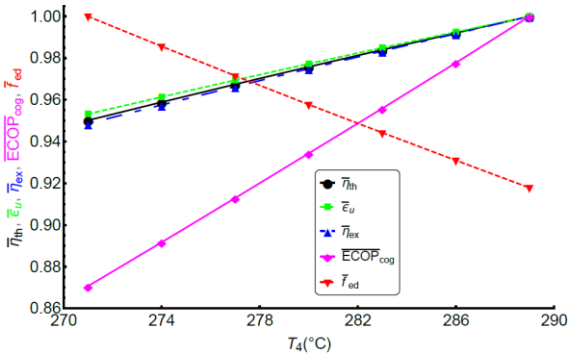

(b)

Figure 2 (Continued). Impact of (a) $\dot{Q}_{SG}$ and (b) T_4 on the objective functions.

The impact of RH mass flow rate ratio and temperature on the energetic and exergetic characteristics of the nuclear desalination plant is illustrated in Figure 3. Higher values of α_{RH} positively affect the performance of the plant. $ECOP_{cog}$ improves by 14.85% as α_{RH} is increased from 0.05 to 0.07. Although the exergy destruction rate of RH increases, FWH1 and FWH2 experience large drops in $\dot{X}_{dest}$ when a higher α_{RH} is chosen, which enhances the plant's performance. The RH temperature, T_{14}, has a relatively less important effect on the objective functions as compared to α_{RH}. Slight decrements are observed in η_{th}, ϵ_u and η_{ex}, and $ECOP_{cog}$ decreases by 3.4% with a 10℃ rise in T_{14}.

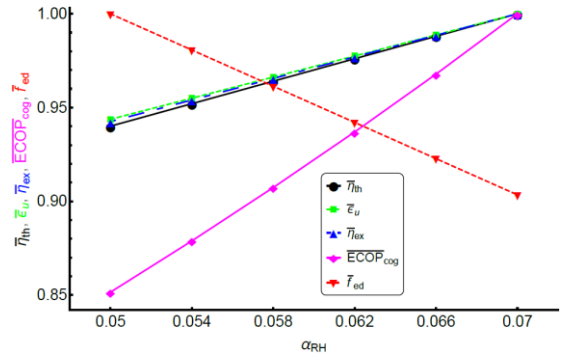

(a)

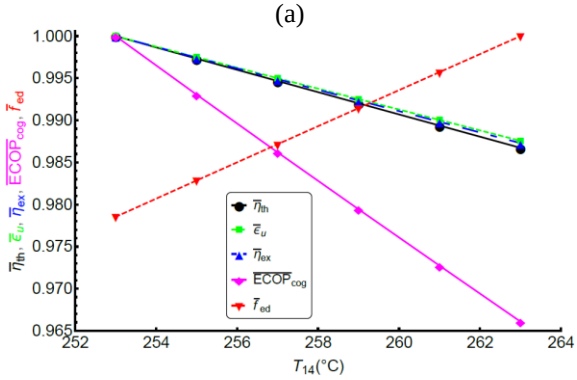

(b)

Figure 3. Variation of performance indicators with (a) α_{RH} and (b) T_{14}.

The effect of desalination capacity on the objective functions of the plant is presented in Figure 4. Increasing $\dot{m}_{72}$ is favorable in terms of ϵ_u, however, it has a negative impact on n_{th}, $ECOP_{cog}$ and f_{ed}. The decrease in thermal efficiency with increasing desalination capacity is a consequence of the drop in electricity output of the cogeneration plant, and such a trend is also shown in [25]. Although an economic analysis is not performed in this study, it should also be noted that increasing the desalination capacity is found to have a positive impact on water cost [28].

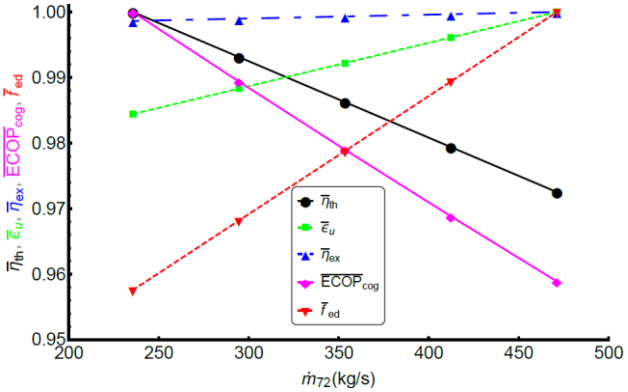

Figure 4. Effect of desalination capacity on the objective functions.

Desalination capacity also affects the plant's performance through the choice of steam extraction node. Tables 5 and 6 demonstrate the variation of the energetic and exergetic performance indicators with steam extraction node for five different desalination capacities, respectively. The desalination capacities given in Tables 5 and 6 correspond to $\dot{m}_{74}$ values of 60, 600, 2400, 3600 and 6000 kg/s. The desalination capacity of $\dot{m}_{72} = 5.9\ kg/s$ corresponds to a small scale plant, 59 kg/s is considered as a large scale plant, and the remaining three capacities are classified as very large scale desalination plants [36]. Results show that the MS outlet (i.e., $i_{ext} = 56$) is the best choice for steam extraction since it gives the optimum values for all objective functions. The selection of extraction node is especially important for very large capacity plants. For instance, based on i_{ext}, η_{th} varies in the range $0.282 - 0.327$ when the desalination capacity is $\dot{m}_{72} = 590\ kg/s$. It should be noted that the choice of steam extraction node might be influenced by economic factors. The exergoeconomic analysis made for SMART driven MSF desalination plant shows that choosing HPT inlet as the steam extraction node results with the least water cost [26].

Table 5. Impact of steam extraction node on energetic objective functions of the nuclear desalination plant for five desalination capacities.

	η_{th}				
i_{ext} \ $\dot{m}_{72}$	$5.9\ kg/s$	$59\ kg/s$	$236\ kg/s$	$353\ kg/s$	$590\ kg/s$
52	0.338030	0.335995	0.329211	0.324688	0.315643
53	0.337697	0.332659	0.315867	0.304673	0.282284
54	0.337725	0.332943	0.317002	0.306375	0.285121
55	0.338129	0.336980	0.333149	0.330596	0.325489
56	0.338146	0.337159	0.333865	0.331670	0.327279
57	0.338105	0.336741	0.332197	0.329167	0.323108
58	0.337715	0.332848	0.316624	0.305807	0.284175
59	0.337795	0.333639	0.319788	0.310554	0.292086
60	0.337817	0.333861	0.320675	0.311884	0.294302
	ϵ_u				
52	0.338392	0.339616	0.343694	0.346413	0.351851
53	0.338059	0.33628	0.33035	0.326398	0.318492
54	0.338087	0.336564	0.331485	0.328100	0.321329
55	0.338491	0.340600	0.347633	0.352321	0.361697
56	0.338509	0.340779	0.348349	0.353395	0.363487
57	0.338467	0.340362	0.346680	0.350892	0.359316
58	0.338078	0.336469	0.331107	0.327532	0.320383
59	0.338157	0.337260	0.334271	0.332279	0.328294
60	0.338179	0.337482	0.335158	0.333609	0.330510

Figure 5 illustrates the variation of the energetic and exergetic characteristics of the nuclear desalination plant with TBT and the MSF unit throttling mass flow rate ratio. Increasing TBT by 35℃ causes a slight decrement in η_{th} and η_{ex} and a more noticeable change of 0.4% in $ECOP_{cog}$ and f_{ed}. However, a higher value of TBT is advantageous in terms of GOR, since this objective function has improved significantly by 34% with a 35℃ increment in TBT. The TBT-GOR relationship presented in Figure 5a is also observed in [15]. The trends shown in Figure 5b reveal that α_{TV2} has a negligible effect on plant's performance. The BH temperature difference (ΔT_{BH}) also affects the GOR of the plant as shown in Figure 6. When ΔT_{BH} rises from 4 to 8, GOR of the facility decreases slightly, and the rate of decrement becomes faster as TBT increases.

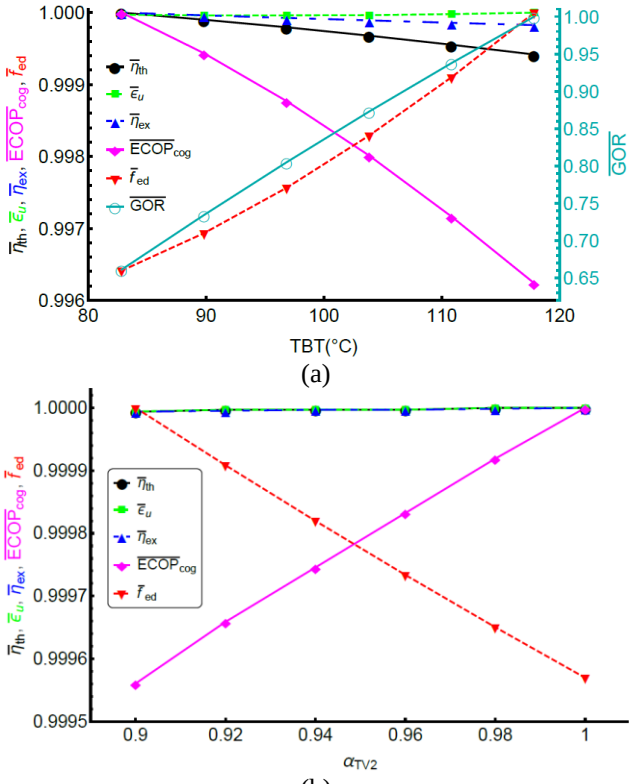

Figure 5. Effect of (a) TBT and (b) TV2 mass flow ratio on the objective functions.

Table 6. Impact of steam extraction node on exergetic objective functions of the nuclear desalination plant for five desalination capacities.

			η_{ex}		
i_{ext} \ $\dot{m}_{72}$	$5.9\ kg/s$	$59\ kg/s$	$236\ kg/s$	$353\ kg/s$	$590\ kg/s$
52	0.641658	0.641856	0.642516	0.642955	0.643834
53	0.640937	0.634639	0.613648	0.599655	0.571667
54	0.640951	0.634781	0.614216	0.600505	0.573085
55	0.641691	0.642178	0.643803	0.644886	0.647052
56	0.641718	0.642454	0.644906	0.646541	0.649810
57	0.641685	0.642123	0.643584	0.644558	0.646506
58	0.640917	0.634441	0.612857	0.598467	0.569687
59	0.640994	0.635210	0.615931	0.603078	0.577373
60	0.640992	0.635194	0.615868	0.602983	0.577214
			$ECOP_{cog}$		
52	1.84323	1.82479	1.76596	1.72887	1.65932
53	1.83784	1.77265	1.57779	1.46422	1.26825
54	1.83816	1.77569	1.58796	1.47785	1.28662
55	1.84430	1.83536	1.80627	1.78746	1.75117
56	1.84456	1.83792	1.81623	1.80214	1.77481
57	1.84405	1.83286	1.79663	1.77335	1.72875
58	1.83797	1.77386	1.58154	1.46898	1.27391
59	1.83898	1.78342	1.61426	1.51346	1.33552
60	1.83919	1.78547	1.62118	1.52278	1.34816
			f_{ed}		
52	0.348117	0.351743	0.363833	0.371892	0.388011
53	0.348744	0.358018	0.388930	0.409538	0.450754
54	0.348691	0.357484	0.386795	0.406336	0.445418
55	0.347932	0.349892	0.356427	0.360783	0.369496
56	0.347898	0.349555	0.355080	0.358763	0.366130
57	0.347976	0.350340	0.358218	0.363470	0.373974
58	0.348709	0.357662	0.387507	0.407404	0.447197
59	0.348560	0.356174	0.381556	0.398477	0.432319
60	0.348518	0.355757	0.379889	0.395976	0.428151

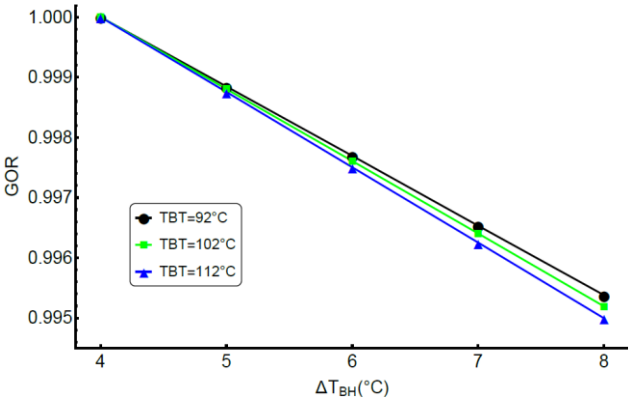

Figure 6. Effect of ΔT_{BH} on GOR of the nuclear desalination plant.

The variation of nuclear desalination plant performance with the seawater temperature and salinity is shown in Figure 7. The temperature and salinity ranges are chosen based on the data of the Mediterranean Sea [37]. The rise in T_0 from 15 ℃ to 27 ℃ has a positive effect on plant's exergetic performance, and the most significant change is observed for $ECOP_{cog}$. On the other hand, an increase in T_0 decreases η_{th} and ϵ_u of the plant relatively by 0.89% and 0.84%, respectively, and such energetic performance degradation is typical for power plants [38]. As for the impact of the seawater salinity, $ECOP_{cog}$ and f_{ed} are found to be the most sensitive objective functions. An increase of 5000 ppm in Sal leads to a relative decrement of 0.13%.

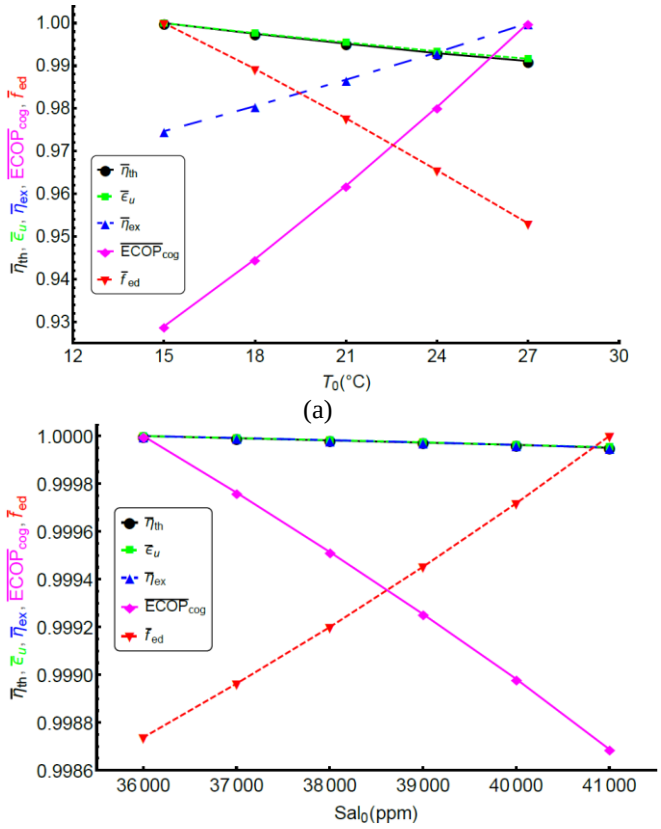

Figure 7. Impact of seawater (a) temperature and (b) salinity on the objective functions.

Based on the results presented in Figures 2-6 together with Tables 5 and 6, an optimum nuclear desalination plant configuration is built to investigate the influence of design decisions on the performance of the nuclear desalination plant by setting $\dot{Q}_{SG} = 3.4\,GW$, $T_4 = 289$℃, $\alpha_{RH} = 0.07$, $T_{14} = 253$℃, $i_{ext} = 56$ and $TBT = 82.85$℃ to produce freshwater with a capacity of $\dot{m}_{72} = 353\,kg/s$ from the seawater having a temperature of $T_0 = 20$℃ and a salinity of $38000ppm$. Thermodynamic properties of all states are presented in Table 7 and 8 for PWR's secondary cycle and desalination facility, respectively. The negative exergy flow rates seen in Table 8 are due to the higher salinity levels of the corresponding states, and such negative values were also reported in [19].

The energetic and exergetic performance indicators of the optimum nuclear desalination plant configuration are presented in Table 9. The performance of a base scenario, for which the results are obtained with the parameters given in Table 3, are also provided in Table 9. Comparison of the results reveal the importance of the parametric energy-exergy analysis of the nuclear desalination plant. All performance indicators except GOR have improved significantly with the alteration of the decision variables. η_{th}, ϵ_u, η_{ex} and $ECOP_{cog}$ increases by 3.01%, 3.15%, 4.70% and 0.46, respectively, and f_{ed} decreases by 5.7% as a result of the alteration of design parameters. The variations correspond to relative improvements of 9.27%, 8.52%, 7.31%, 26.63% and 15.27% in η_{th}, ϵ_u, η_{ex}, $ECOP_{cog}$ and f_{ed}, respectively These improvements are significant. The findings can also be interpreted from an economic perspective. For instance, the price of electricity is $0.1235\,\$/kWh$ for the Akkuyu nuclear power plant that is under construction in Mersin, Turkey for which a single reactor unit has a nominal power output of $1200MW$. A 3.01% increase in thermal efficiency can be considered as a $36MW$ improvement in the power output. Nuclear power plants have an average capacity factor of 90%. Therefore, the 3.01% increase in thermal efficiency would cause a 35.05 million $ yearly improvement in the revenue of the plant.

Table 7. Thermodynamic properties of all states for the secondary cycle of the PWR.

State	T(℃)	$P(MPa)$	$\dot{m}(kg/s)$	$h(kJ/kg)$	$s(kJ/kg\cdot K)$	$\dot{X}(MW)$
4	289.00	7.334	1899.62	2768.17	5.7910	2039.31
5	289.00	7.334	1766.64	2768.17	5.7910	1896.58
6	289.00	7.334	132.97	2768.17	5.7910	142.75
7	226.05	2.600	104.48	2606.30	5.8482	93.50
8	201.37	1.600	94.98	2535.45	5.8775	77.45
9	184.86	1.120	1567.18	2485.54	5.8999	1189.47
10	184.86	1.120	1567.18	2485.54	5.8999	1189.47
11	184.86	1.120	1335.00	2781.36	6.5457	1155.41
12	184.86	1.120	1299.15	2781.36	6.5457	1124.38
13	253.00	1.120	1299.15	2945.36	6.8804	1209.98
14	253.00	1.120	1299.15	2945.36	6.8804	1209.98
15	228.52	0.880	75.98	2899.96	6.8991	66.90
16	147.90	0.450	64.59	2706.82	6.7692	46.85

Table 7 (Continued). Thermodynamic properties of all states for the secondary cycle of the PWR.

State	$T(℃)$	$P(MPa)$	$\dot{m}(kg/s)$	$h(kJ/kg)$	$s(kJ/kg \cdot K)$	$\dot{X}(MW)$
17	120.21	0.200	64.59	2666.43	7.0257	39.39
18	96.73	0.090	64.59	2559.37	7.0942	31.18
19	69.09	0.030	49.39	2427.14	7.1905	15.91
20	30.03	0.004	980.01	2226.51	7.3661	68.74
21	20.00	0.101	99559.60	83.91	0.2965	0.00
22	20.03	0.200	99559.60	84.03	0.2968	0.60
23	25.03	0.101	99559.60	104.95	0.3676	17.97
24	30.03	0.004	1015.87	125.86	0.4372	0.70
25	30.03	0.030	1015.87	125.89	0.4373	0.70
26	55.55	0.030	1065.26	232.58	0.7751	8.91
27	55.57	0.090	1065.26	232.65	0.7753	8.92
28	87.29	0.090	1129.85	365.66	1.1614	31.84
29	87.32	0.200	1129.85	365.79	1.1618	31.86
30	116.79	0.200	1194.44	490.20	1.4932	66.24
31	116.87	0.450	1194.44	490.51	1.4940	66.33
32	143.50	0.450	1259.03	604.20	1.7754	109.20
33	143.63	0.880	1259.03	604.75	1.7767	109.41
34	184.86	0.880	232.18	784.58	2.1862	34.06
35	266.20	7.334	132.97	1165.85	2.9405	40.80
36	215.64	0.880	365.15	923.42	2.4983	70.86
37	182.87	0.880	1700.16	775.77	2.1670	243.98
38	183.09	1.600	1700.16	776.73	2.1691	244.57
39	203.88	1.600	1795.14	869.78	2.3670	321.11
40	204.18	2.600	1795.14	871.15	2.3699	322.07
41	226.05	2.600	1899.62	966.59	2.5736	408.68
42	227.48	7.334	1899.62	978.33	2.5868	423.63
43	289.00	7.334	1899.62	2768.17	5.7910	2039.31
44	226.05	2.600	104.48	2606.30	5.8482	93.50
45	201.37	1.600	94.98	2535.45	5.8775	77.45
46	228.52	0.880	75.98	2899.96	6.8991	66.90
47	147.90	0.450	64.59	2706.82	6.7692	46.85
48	120.21	0.200	64.59	2666.43	7.0257	39.39
49	96.73	0.090	64.59	2559.37	7.0942	31.18
50	69.09	0.030	49.39	2427.14	7.1905	15.91
51	30.03	0.004	980.01	2226.51	7.3661	68.74
52	289.00	7.334	0.00	2768.17	5.7910	0.00
53	226.05	2.600	0.00	2606.30	5.8482	0.00
54	201.37	1.600	0.00	2535.45	5.8775	0.00
55	184.86	1.120	0.00	2485.54	5.8999	0.00
56	184.86	1.120	35.85	2781.36	6.5457	31.03
57	253.00	1.120	0.00	2945.36	6.8804	0.00
58	228.52	0.880	0.00	2899.96	6.8991	0.00
59	147.90	0.450	0.00	2706.82	6.7692	0.00
60	120.21	0.200	0.00	2666.43	7.0257	0.00
61	96.73	0.090	0.00	2559.37	7.0942	0.00
62	69.09	0.030	0.00	2427.14	7.1905	0.00
63	30.03	0.004	0.00	2226.51	7.3661	0.00
64	184.86	1.120	35.85	784.58	2.1862	5.26
65	30.02	0.004	35.85	784.58	2.6010	0.81
66	88.85	0.067	31.33	2657.73	1.1796	472.53
67	88.85	0.067	31.33	372.20	0.3811	37.80

Table 8. Thermodynamic properties of all states for the MSF facility.

State	$T(℃)$	$P(MPa)$	$Sal(ppm)$	$\dot{m}(kg/s)$	$h(kJ/kg)$	$s(kJ/kg \cdot K)$	$\dot{X}(MW)$
68	20.00	0.168	38000	1455.88	81.99	0.3183	0.09
69	28.00	0.118	38000	1455.88	114.38	0.4275	0.66
70	28.00	0.118	38000	689.63	114.38	0.4275	0.31
71	28.00	0.010	38000	689.63	114.38	0.4275	0.30
72	26.00	0.010	0.01	315.26	109.02	0.3812	2.72
73	28.00	0.010	70000	374.37	111.68	0.4366	-1.85
74	28.00	0.010	65000	3600.00	112.09	0.4354	-15.00
75	28.00	0.635	65000	3600.00	112.62	0.4352	-12.89
76	77.85	0.635	65000	3600.00	310.29	1.0426	57.74
77	82.85	0.635	65000	3600.00	330.18	1.0988	69.96
78	26.00	0.578	0.01	315.26	109.54	0.3811	2.90
79	28.00	0.292	70000	374.37	111.92	0.4366	-1.75
80	20.00	0.101	70000	374.37	80.18	0.3303	-1.97
81	20.00	0.101	0.01	315.26	84.01	0.2965	2.67
82	20.00	0.101	38000	766.25	81.93	0.3183	0.00

Table 9. Comparison of an optimum configuration with a base configuration for the nuclear desalination plant.

Performance indicator	Base scenario	Optimum scenario
η_{th}	0.3247	0.3548
ϵ_u	0.3464	0.3759
GOR	11.1781	10.0639
η_{ex}	0.6429	0.6899
$ECOP_{cog}$	1.7289	2.1893
f_{ed}	0.3719	0.3151

The irreversibility rates of plant components are presented in Figs. 8 and 9 for PWR's secondary cycle and MSF facility, respectively. Secondary cycle of the PWR has a total irreversibility rate of $551.75 MW$ and SG has the largest contribution of 32%. The total exergy destruction rate of the MSF facility, $13.10\ MW$ is low as compared to the secondary cycle and the MSF unit is responsible for the majority of the losses. Results of [19] also show that MSF unit is the largest source of irreversibility in the desalination facility.

5. Conclusion

Access to freshwater is a challenging issue for regions with arid climate. Desalination is an essential technology for countries having water scarcity problems and nuclear energy is a promising source that can provide both thermal and electrical energy for desalination facilities with a negligible environmental impact. This study focuses on a comprehensive energy and exergy analysis of a nuclear desalination plant. A pressurized water reactor is used as the energy source to produce electricity and to supply process heat to a multi-stage flash desalination facility for seawater desalination. The effects of several design and operating parameters on the energetic and exergetic characteristics of the plant are studied in detail. The results of the analysis can be summarized as follows:

- Higher reactor thermal power has a positive impact on thermal efficiency, coefficient of ecological performance and exergy destruction factor of the plant, while it tends to decrease utilization factor.
- The overall plant performance improves as the live steam temperature and the reheater mass flow rate ratio increase, while a lower reheater temperature is preferable for better cogeneration performance.
- Increasing the freshwater production capacity improves the utilization factor of the nuclear desalination plant, on the other hand, it has a negative impact on thermal efficiency, coefficient of ecological performance and exergy destruction factor.
- The outlet of the moisture separator is the best candidate for steam extraction, and the selection of

extraction node is crucial for very large scale desalination plants.

- Gain output ratio of the plant enhances remarkably with increasing top brine temperature. Decreasing the brine heater temperature difference also has a positive impact on the gain output ratio, and the throttling valve mass flow rate ratio has a negligible effect on plant's performance.
- A higher seawater temperature tends to decrease the energetic performance of the nuclear desalination plant, however, it positively affects the exergetic objective functions. A higher seawater salinity causes a slight decrement in the exergetic performance.
- The overall plant performance can be significantly improved by carefully selecting the design parameters.
- Steam generator and multi-stage flash unit cause the largest exergy destruction rates in the secondary cycle of the reactor and multi-stage flash facility, respectively.

The findings of this study provide useful technical information for both the designers of PWR based nuclear desalination systems and policy makers, especially in countries suffering from water scarcity. With that being said, the detailed analysis presented in this paper can be further improved by considering economic factors and carrying out a multiobjective optimization that takes into account energetic, exergetic and economic objective functions. Research into performing this optimization is already in progress.

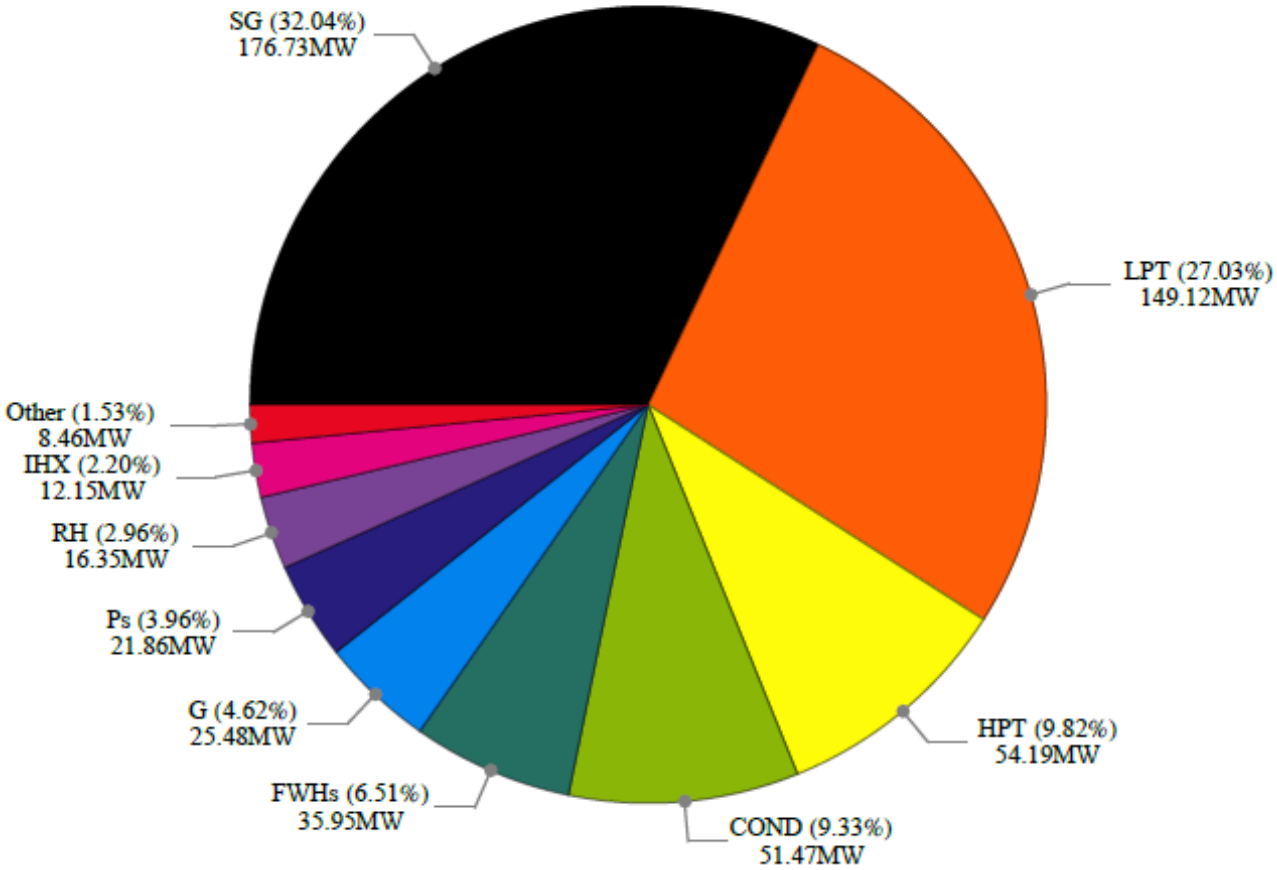

Figure 8. Exergy destruction rates of PWR's secondary cycle components.

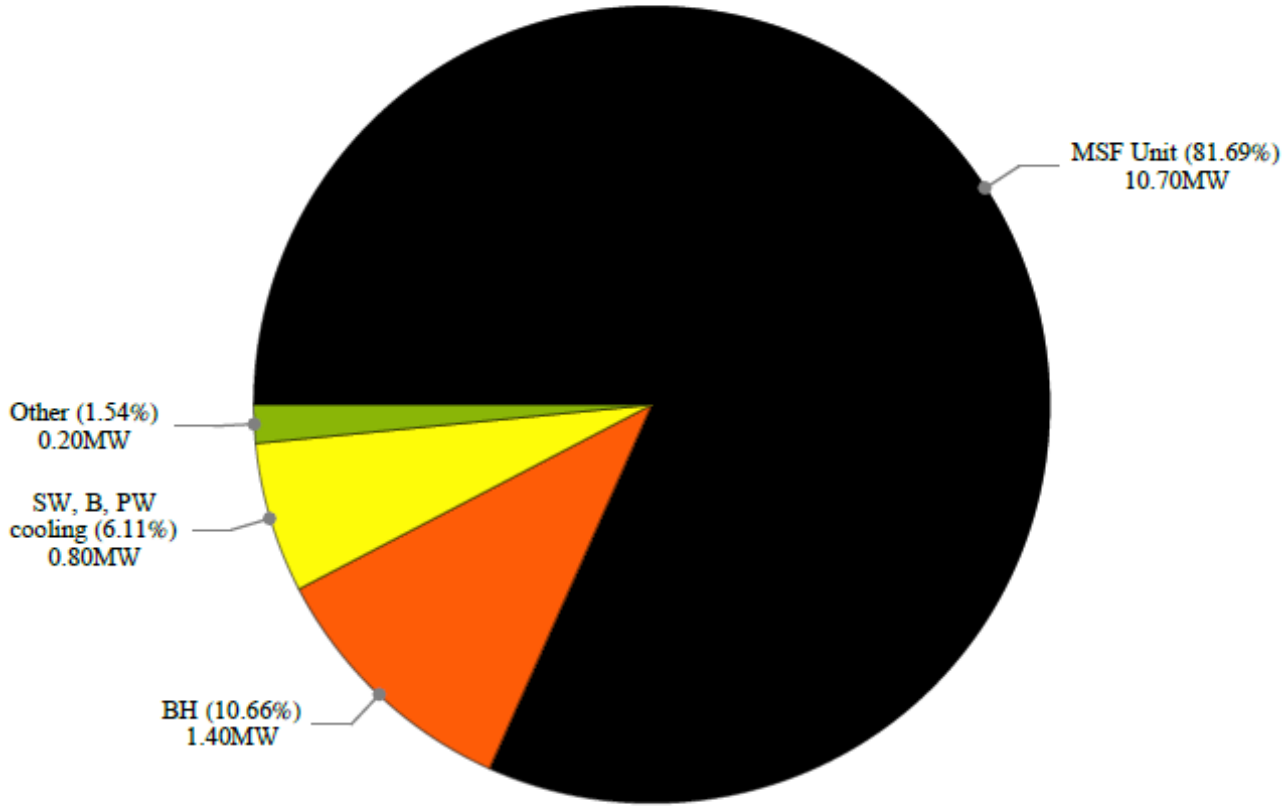

Figure 9. Exergy destruction rates of MSF facility components.

Contributions of The Authors

Akyürek: Literature review, Formal analysis, Validation, Writing – original draft
Tanbay: Conceptualization, Formal analysis, Methodology, Software development, Supervision, Visualization, Writing – review and editing

Conflict of Interest Statement

There is no conflict of interest between the authors.

Statement of Research and Publication Ethics

The study is complied with research and publication ethics.

References

[1] IAEA, "Introduction of Nuclear Desalination," International Atomic Energy Agency, Vienna, Austria, Technical Reports Series no. 400, 2000.

[2] IAEA, "Status of Nuclear Desalination in IAEA Member States," International Atomic Energy Agency, Vienna, Austria, IAEA-TECDOC-1524, 2007.

[3] FAO and UN Water, "Progress on Level of Water Stress. Global status and acceleration needs for SDG Indicator 6.4.2," United Nations, Rome, Italy, 2021.

[4] M. A. Rosen, "Nuclear Energy: Non-Electric Applications," *Eur. J. Sust. Dev. Res.*, vol. 5, no. 1, 2021, Art. no. em0147.

[5] EIA, "Electric Power Monthly," EIA. Accessed: Feb. 5, 2024. [Online]. Available: https://www.eia.gov/electricity/monthly/epm_table_grapher.php?t=epmt_6_07_b

[6] A. Panagopoulos, and K. J. Haralambous, "Environmental impacts of desalination and brine treatment - Challenges and mitigation measures," *Mar. Pollut. Bull.*, 2020, vol. 161, Dec. 2020, Art. no. 111773.

[7] R. S. El-Emam, H. Ozcan, R. Bhattacharyya, and L. Awerbuch, "Nuclear desalination: A sustainable route to water security," *Desalination*, vol. 542, Nov. 2022, Art. no. 116082.

[8] M. Ayaz, M. A. Namazi, M. Ammad ud Din, M. I. M. Ershath, A. Mansour, and E. M. Aggoune, "Sustainable seawater desalination: Current status, environmental implications and future expectations," *Desalination*, vol. 540, Oct. 2022, Art. no. 116022.

[9] H. Nassrullah, S. F. Anisa, R. Hashaikeh, and N. Hilal, "Energy for desalination: A state-of-the-art review," *Desalination*, vol. 491, Oct. 2020, Art. no. 114569.

[10] D. Curto, V. Franzitta, and A. Guercio, "A review of the water desalination technologies," *Appl. Sci.*, vol. 11, no. 2, Jan. 2021, Art. no. 670.

[11] I. G. Sánchez-Cervera, K. C. Kavvadias, and I. Khamis, "DE-TOP: A new IAEA tool for the thermodynamic evaluation of nuclear desalination," *Desalination*, vol. 321, pp. 103-109, Jul. 2013.

[12] K. C. Kavvadias, and I. Khamis, "The IAEA DEEP desalination economic model: A critical review," *Desalination*, vol. 257, pp. 150-157, Jul. 2010.

[13] R. S. Faibish, and H. Ettouney, "MSF nuclear desalination," *Desalination*, vol. 157, pp. 277-287, Aug. 2003.

[14] S. Ghurbal, and M. Ashour, "Economic competitiveness of nuclear desalination in Libya," *Desalination*, vol. 158, pp. 201-204, Aug. 2003.

[15] D. T. Ingersoll, J. L. Binder, D. Conti, and M. E. Ricotti, "Nuclear desalination option for the international reactor innovative and secure (IRIS) design," presented at 5th International Conference on Nuclear Option in Countries with Small and Medium Electricity Grids, Dubrovnik, Croatia, May 16-20, 2004.

[16] A. K. Adak, and P. K. Tewari, "Coupling aspects of an MSF desalination plant and loss of electrical power generation of a nuclear power plant: case study," *Int. J. Nucl. Desalin.*, vol. 1, no. 3, pp. 373-381, Oct. 2004.

[17] A. K. Adak, V. K. Srivastava, and P. K. Tewari, "Thermal coupling system analysis of a nuclear desalination plant," *Int. J. Nucl. Desalin.*, vol. 4, no. 2, pp. 123-133, Sep. 2010.

[18] L. Tian, J. Guo, Y. Tang, and L. Cao, "A historical opportunity: economic competitiveness of seawater desalination project between nuclear and fossil fuel while the world oil price over $50 per boe-part A: MSF," *Desalination*, vol. 183, pp. 317-325, Nov. 2005.

[19] N. Kahraman and Y. A. Cengel, "Exergy analysis of a MSF distillation plant," *Energ. Convers. Manage*, vol. 46, no. 15-16, pp. 2625-2636, Sep. 2005.

[20] M. S. Saadawy, "Optimum thermal coupling system for co-generation nuclear desalination plants," *Int. J. Nucl. Desalin.*, vol. 2, no. 1, pp. 22-43, Apr. 2006.

[21] M. H. K. Manesh, and M. Amidpour, "Multi-objective thermoeconomic optimization of coupling MSF desalination with PWR nuclear power plant through evolutionary algorithms," *Desalination*, vol. 249, no. 3, pp. 1332-1344, Dec. 2009.

[22] M. H. K. Manesh, M. Amidpour, and M. H. Hamedi, "Optimization of the coupling of pressurized water nuclear reactors and multistage flash desalination plant by evolutionary algorithms and thermoeconomic method," *Int. J. Energ. Res.*, vol. 33, no. 1, pp. 77-99, 2009.

[23] G. Alonso, S. Vargas, E. del Valle, and R. Ramirez, "Alternatives of seawater desalination using nuclear power," *Nucl. Eng. Des.*, vol. 245, pp. 39-48, Apr. 2012.

[24] X. Yan, H. Noguchi, H. Sato, Y. Tachibana, K. Kunitomi, and R. Hino, "Study of an incrementally loaded multistage flash desalination system for optimum use of sensible waste heat from nuclear power plant," *Int. J. Energ. Res.*, vol. 37, no. 14, pp. 1811-1820, 2013.

[25] D. T. Ingersoll, Z. J. Houghton, R. Bromm, and C. Desportes, "NuScale small modular reactor for Co-generation of electricity and water," *Desalination*, vol. 340, pp. 84-93, May 2014.

[26] E. Priego, G. Alonso, E. del Valle, and R. Ramirez, "Alternatives of steam extraction for desalination purposes using SMART reactor," *Desalination*, vol. 413, pp. 199-216, Jul. 2017.

[27] S. U. D. Khan, S. U. D. Khan, S. Haider, A. El-Leathy, U. A. Rana, S. N. Danish and R. Ullah, "Development and techno-economic analysis of small modular nuclear reactor and desalination system across Middle East and North Africa region," *Desalination*, vol. 406, pp. 51-59, Mar. 2017.

[28] S. U. D. Khan, and S. U. D. Khan, "Karachi Nuclear Power Plant (KANUPP): As case study for techno-economic assessment of nuclear power coupled with water desalination," *Energy*, vol. 127, pp. 372-380, May 2017.

[29] M. F. Polat, and I. Dincer, "Comparative evaluation of possible desalination options for Akkuyu Nuclear Power Plant," in *Exergetic, Energetic and Environmental Dimensions*, I. Dincer, C. O. Colpan, and O. Kizilkan, Eds., Academic Press, 2018, pp. 583-596.

[30] E. Dewita, T. Ariyanto, H. Susiati, and M. Pancoko, "Conceptual design of Indonesia experimental power reactor coupled with desalination unit," *J. Phys. Conf. Ser.*, vol. 1198, no. 2, 2019, Art. no. 022056.

[31] K. Sadeghi, S. H. Ghazaie, E. Sokolova, E. Fedorovich, and A. Shirani, "Comprehensive techno-economic analysis of integrated nuclear power plant equipped with various hybrid desalination systems," *Desalination*, vol. 493, Nov. 2020, Art. no. 114623.

[32] E. K. Redfoot, M. G. McKellar, and R. A. Borrelli, "Allocating heat and electricity in an Integrated Energy System coupled with a water purification system," *Nucl. Eng. Des.*, vol. 397, Oct. 2022, Art. no. 111902.

[33] A. Al Ghamdi, and I. Mustafa, "Exergy analysis of a MSF desalination plant in Yanbu, Saudi Arabia," *Desalination*, vol. 399, pp. 148-158, Dec. 2016.

[34] B. Najafi, A. Shirazi, M. Aminyavari, F. Rinaldi, and R. A. Taylor, "Exergetic, economic and environmental analyses and multi-objective optimization of an SOFC-gas turbine hybrid cycle coupled with an MSF desalination system," *Desalination*, vol. 334, no. 1, pp. 46-59, Feb. 2014.

[35] M. W. Chase, "NIST-JANAF thermochemical tables 2 volume set," in *Journal of physical and chemical reference data monographs*. College Park, MD: American Institute of Physics, 1998.

[36] A. N. Bdour, N. Al-Sadeq, M. Gharaibeh, A. Mendoza-Sammet, M. D. Kennedy, and S. G. Salinas-Rodriguez, "Techno-economic analysis of selected PV-BWRO desalination plants in the context of the water-energy nexus for low-medium-income countries," *Energies*, vol. 15, no. 22, Nov. 2022, Art. no. 8657.

[37] S. C. Painter, and M. N. Tsimplis, “Temperature and salinity trends in the upper waters of the Mediterranean Sea as determined from the MEDATLAS dataset,” *Cont. Shelf Res.*, vol. 23, no. 16, pp. 1507-1522, Oct. 2003.

[38] A. Durmayaz, and O. S. Sogut, “Influence of cooling water temperature on the efficiency of a pressurized-water reactor nuclear-power plant,” *Int. J. Energ. Res.*, vol. 30, no. 10, pp. 799-810, Apr. 2006.